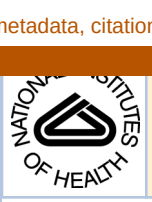

Published in final edited form as:

Bioorg Med Chem Lett. 2013 September 15; 23(18): 5209–5212. doi:10.1016/j.bmcl.2013.06.093.

Extension into the entrance channel of HIV-1 reverse transcriptase – crystallography and enhanced solubility

Mariela Bollini[a], **Kathleen M. Frey**[b], **José A. Cisneros**[a], **Krasimir A. Spasov**[b], **Kalyan Das**[c], **Joseph D. Bauman**[c], **Eddy Arnold**[c], **Karen S. Anderson**[b], and **William L. Jorgensen**[a]

[a]Department of Chemistry, Yale University, New Haven, CT 06520-8107, USA

[b]Department of Pharmacology, Yale University School of Medicine, New Haven, CT 06520-8066, USA

[c]Department of Chemistry and Chemical Biology, Rutgers University, Piscataway, NJ 08854, USA

Abstract

Non-nucleoside inhibitors of HIV-1 reverse transcriptase (HIV-RT) are reported that feature extension into the entrance channel near Glu138. Complexes of the parent anilinylpyrimidine **1** and the morpholinoethoxy analog **2j** with HIV-RT have received crystallographic characterization confirming the designs. Measurement of aqueous solubilities of **2j**, **2k**, the parent triazene **2a**, and other NNRTIs demonstrate profound benefits for addition of the morpholinyl substituent.

Non-nucleoside inhibitors of HIV-1 reverse transcriptase (NNRTIs) are a central component of anti-HIV therapy.[1] There are five FDA-approved drugs in the class: nevirapine, delavirdine, efavirenz, etravirine, and rilpivirine. In view of the rapid mutation of the virus, NNRTIs are given in combination therapies. Though the class has demonstrated important utility, further improvements are possible to address issues of safety, administration, and virologic failure.[2–4] There is also need to be positioned to respond to the emergence of pan-resistant viral variants and unknown effects of long-term treatment.[5]

Our efforts at Yale to discover new series of NNRTIs have combined computer-aided design, synthesis, and biological assaying.[6,7] For two picomolar inhibitors, which feature a catechol diether substructure,[8] we also recently reported X-ray crystal structures for their complexes with wild-type (WT) HIV-RT.[9] One of the earliest series that we had investigated was anilinylazines containing a dimethylallyloxy substituent. This work culminated in the pyrimidine **1** and the corresponding 1,3,5-triazine (**2a**), which yield EC_{50} values of 2 and 11 nM in a standard assay using MT-2 cells infected with WT HIV-1.[10] Though results of molecular modeling, starting from the 1S9E crystal structure of an anilinyltriazene,[11] were reported for complexes of the inhibitors with HIV-RT, the binding mode for **1** was confirmed by an X-ray crystal structure. This structure, which was obtained by the Rutgers group, is reported here and illustrated in Figures 1 and 2.[12]

Consistent with the 1S9E structure and the modeling, **1** resides in the NNRTI binding site with the hydrophobic dimethylallyl group positioned in the π-box formed by Tyr181,

Tyr188, Phe227, and Trp229 (Figure 1). There are also hydrogen bonds between the backbone O and N of Lys101 and the amidine moiety of **1**, which are clearer from the orthogonal view in Figure 2. This Figure also highlights a salt bridge between the side chains of Glu138 and Lys101, a feature that is not always found in NNRTI complexes, e.g., the 1S9E structure.[11] The X-ray results provide important validation of the structure-activity patterns that were obtained for **1** and its analogs.[10] This includes rationalization of the poor activity of these compounds towards viral variants containing the clinically important Tyr181Cys mutation owing to the substantial contact of Tyr181 with the dimethylallyl group of **1**.[10,14]

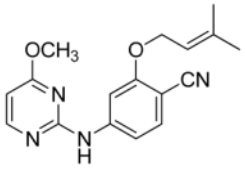

1

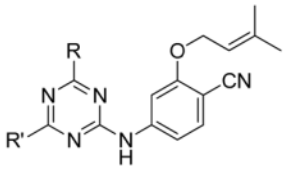

2

Subsequent efforts included the probing of relatively unexplored regions including the ‘eastern channel’ or ‘groove’[15] extending back and down from the cyano group of **1** in Figure 1 and the ‘entrance channel’ extending into the solvent-exposed region to the left of Lys101 in Figure 2.[16] The intentions were to seek extensions that might (1) improve potency towards both WT HIV-1 and variants containing common NNRTI-induced point mutations, and/or (2) improve physical properties of the NNRTIs. Extension into the entrance channel for **1** and **2** would require attachment of a substituent at C6 of the azine rings (Figure 1). It was not clear that this would be successful owing to possible unfavorable contacts, especially with Glu138 (Figure 2). However, the idea was pursued and it was found that substantial substituents could be attached at this position, though with some loss of potency.[16] For example, as summarized in Table 1, the methoxyethoxy and methoxytriethoxy containing **2c** and **2e** yield EC_{50} values of 97 and 380 nM in the MT-2 cell assay, while the parent **2a** and dimethoxy analog **2b** are 11- and 22-nM inhibitors. It was even found that large, dimeric NNRTIs could be accommodated, e.g., **3** gives an EC_{50} of 170 nM.[16]

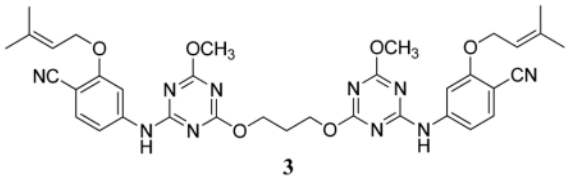

3

The present report extends the investigations of the entrance channel. Additional compounds were synthesized and assayed, specifically, the amino-terminating **2f** and **2g** and the morpholinoethoxy and -propoxy analogs **2j** – **2m**. The latter compounds were prepared as before via S_NAr reactions of alkoxides with the intermediate **4**;[16] however, an alternative route was necessary for the amines (Scheme 1). The S_NAr reaction was performed earlier in the sequence to install the side chain on dichloromethoxytriazene, and the amino group was unmasked in the last step.

In the same manner as in previous reports,[6–10,14–16] activities against the IIIB strain of HIV-1 were measured using MT-2 human T-cells; EC_{50} values are obtained as the dose required to achieve 50% protection of the infected cells by the MTT colorimetric method. Simultaneously, CC_{50} values for inhibition of MT-2 cell growth by 50% are obtained. The

identity of all assayed compounds was confirmed by ^{1}H and ^{13}C NMR and high-resolution mass spectrometry; purity was >95% as judged by high-performance liquid chromatography.

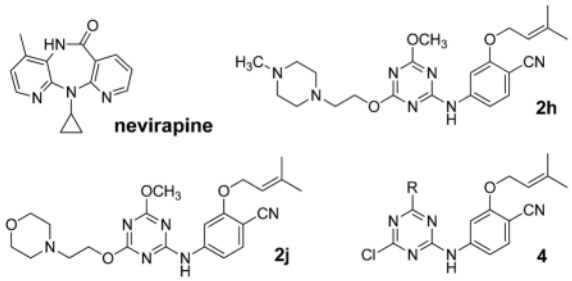

The amines **2f** and **2g** were of interest to test the effects of a positive charge at the end of the side chains and increases in length beyond **2e**. The results for **2f** and **2g** in Table 1 show that these modifications are not beneficial for activity. The interest in the morpholine containing compounds was particularly high since this modification would likely improve the solubility of the compounds. Poor solubility has often been an issue in NNRTI development, stemming from the hydrophobic character of the NNRTI binding site.[1,16–19] Thus, it was pleasing to find good activity for **2j** (92 nM) and **2k** (95 nM). This represents significant improvement over the methylpiperazinyl and THP analogs **2h** and **2i**.

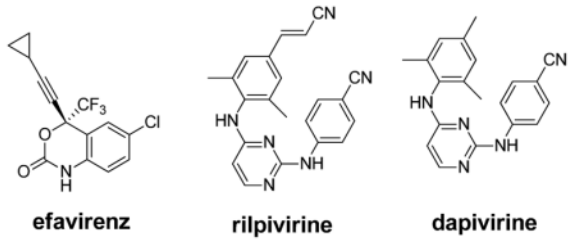

Furthermore, we quantified the aqueous solubilities of **2a**, **2j**, **2k**, dapivirine (TMC120), and efavirenz using a shake-flask method with UV detection (Agilent 8453).[21] The results in Table 2, which also includes previous reports for rilpivirine, are striking. Addition of the morpholinoalkoxy substituent to **2a** to yield **2j** or **2k** delivers a 400 to 500-fold improvement in solubility. The results for **2j** and **2k** are similar to that for evafirenz and place them within the normal range observed for oral drugs.[22] In contrast, the sub-μg/mL solubilities for dapivirine and rilpivirine are well outside the normal range. Though rilpivirine is an FDA-approved oral drug, it likely has an unusual absorption mechanism involving aggregates,[23] while dapivirine is being pursued as a vaginal microbicide.[24] Thus, compounds **2j** and **2k** have good aqueous solubility and potencies similar to that of nevirapine. Though their activities in the WT cell assay are 100-fold less than for rilpivirine or dapivirine, their solubilities are 175 to 350-fold greater.

Finally, to confirm the expectation of the placement of the morpholinoethoxy side chain in the entrance channel and to elucidate its contacts, a co-crystal structure of **2j** and WT HIV-RT was pursued by the investigators at Yale using similar methods as previously reported.[9] Crystals with the recombinant RT52A enzyme were obtained that diffracted to 2.9-Å resolution, data were collected at the Brookhaven NSLS on beam line X25, and the structure was solved by molecular replacement using the 2ZD1 structure of rilpivirine with HIV-RT[25] as the search model. The electron density for the non-nucleoside binding region is ordered and provides clear characterization of the interactions with the inhibitor (Figure 3). An alternative rendering of the structure is provided in Figure 4.

The positioning of **2j** in the NNRTI binding site is the same as for **1** including the hydrogen bonds with Lys101 and the placement of the dimethylallyl group in the **π**-box; however, the salt bridge between Glu138 and Lys101 is no longer present (Figure 4). Overall, the co-crystal structures reported here for **1** and **2j** have an rmsd of only 1.4 Å for an all-atom alignment. Since the contact between Tyr181 and the dimethylallyl group is retained, **2j** does not show activity towards the Y181C-containing viral variant. Most notably, the structure for **2j** confirms the anticipated extension of the morpholinoethoxy side chain into the entrance channel towards Glu28. The carboxylate group of Glu138 contacts the carbon atoms of the ethoxy subunit with O-C separations of 2.8 – 3.6 Å. The carboxylate oxygens are also 3.8 and 4.4 Å from the morpholine nitrogen, which is presumably protonated. In addition, the morpholine oxygen is proximal to the carboxylate carbon (4.1 Å) and oxygens (3.4 and 4.3 Å) of Glu28.

Though it might seem that replacement of the oxygen of the morpholine with a positively charged group would enhance binding, beneficial effects were not apparent for the 4-methylpiperazinyl analog **2h** (Table 1). In this case, only one of the tertiary nitrogens would be protonated near pH 7, since the pK_a values for 1,4-dimethylpiperazine are 8.4 and 3.8.[26] Thus, a favorable electrostatic interaction with either Glu138 or Glu28 has to be sacrificed.

In summary, with compounds **2j** and **2k** it has been demonstrated that it is possible to extend anilinylazine NNRTIs into the entrance channel of the NNRTI binding site to achieve profound improvements in aqueous solubility. **2j** and **2k** are similar in anti-HIV activity to the drug nevirapine, but they have 200 to 500-fold greater solubility than the parent compound **2a** and the diarylpyrimidines dapivirine and rilpivirine. Analogous application of the present approach to the latter series of compounds may be expected to yield similar benefits for solubility, while hopefully retaining their excellent activity towards viral variants.

Acknowledgments

Gratitude is expressed to the National Institutes of Health (AI27690, AI44616, GM32136, GM49551) for research support and fellowship support for K. M. F. (AI104334). Receipt of reagents through the NIH AIDS Research and Reference Reagent Program, Division of AIDS, NIAID, NIH is also greatly appreciated.

References

1. de Bethune MP. Antiviral Res. 2010; 85:75. [PubMed: 19781578]
2. Chiao SK, Romero DL, Johnson DE. Curr Opin Drug Disc Dev. 2009; 12:53.
3. Adams J, Patel N, Mankaryous N, Tadros M, Miller CD. Ann Pharmacotherapy. 2010; 44:157.
4. Molina JM, Cahn P, Grinsztejn B, Lazzarin A, Mills A, Saag M, Supparatpinyo K, Walmsley S, Crauwels H, Rimsky LT, Vanveggel S, Boven K. Lancet. 2011; 378:238. [PubMed: 21763936]
5. Richman DD, Margolis DM, Delaney M, Greene WC, Hazuda D, Pomerantz RJ. Science. 2009; 323:1304. [PubMed: 19265012]
6. Jorgensen WL, Ruiz-Caro J, Tirado-Rives J, Basavapathruni A, Anderson KS, Hamilton AD. Bioorg Med Chem Lett. 2006; 16:663. [PubMed: 16263277]
7. Jorgensen WL. Acc Chem Res. 2009; 42:724. [PubMed: 19317443]
8. Bollini M, Domaoal RA, Thakur VV, Gallardo-Macias R, Spasov KA, Anderson KS, Jorgensen WL. J Med Chem. 2011; 54:8582. [PubMed: 22081993]
9. Frey KM, Bollini M, Mislak AC, Cisneros JA, Gallardo-Macias R, Jorgensen WL, Anderson KA. J Am Chem Soc. 2012; 134:19501. [PubMed: 23163887]
10. Thakur VV, Kim JT, Hamilton AD, Bailey CM, Domaoal RA, Wang L, Anderson KS, Jorgensen WL. Bioorg Med Chem Lett. 2006; 16:5664. [PubMed: 16931015]

11. Das K, Clark AD Jr, Lewi PJ, Heeres J, de Jonge MR, Koymans LMH, Vinkers HM, Daeyaert F, Ludovici DW, Kukla MJ, De Corte B, Kavash RW, Ho CY, Ye H, Lichtenstein MA, Andries K, Pauwels R, de Béthune MP, Boyer PL, Clark P, Hughes SH, Janssen PAJ, Arnold E. J Med Chem. 2004; 47:2550. [PubMed: 15115397]
12. RT (crystal engineered mutant RT52A) was expressed, purified, and co-crystallized with 1, as previously described.[13] Data collection was performed at the Cornell High Energy Synchrotron Source (CHESS) F1 beamline. The diffraction data was processed and scaled using HKL2000. The structure was refined to 1.95-Å resolution to R and R-free of 0.237 and 0.275, respectively, using PHENIX. The atomic coordinates and structure factors are deposited in the PDB with ID 4KO0.
13. Bauman JD, Das K, Ho WC, Baweja M, Himmel DM, Clark AD Jr, Oren DA, Boyer PL, Hughes SH, Shatkin AJ, Arnold E. Nucleic Acids Res. 2008; 36:5083. [PubMed: 18676450]
14. Jorgensen WL, Bollini M, Thakur VV, Domaoal RA, Spasov K, Anderson KS. J Am Chem Soc. 2011; 133:15686. [PubMed: 21853995]
15. Leung CS, Zeevaart JG, Domaoal RA, Bollini M, Thakur VV, Spasov K, Anderson KS, Jorgensen WL. Bioorg Med Chem Lett. 2010; 20:2485. [PubMed: 20304641]
16. Ekkati AR, Bollini M, Domaoal RA, Spasov KA, Anderson KS, Jorgensen WL. Bioorg Med Chem Lett. 2012; 22:1565. [PubMed: 22269110]
17. Ojewole E, Mackraj I, Naidoo P, Govender T. Eur J Pharm Biopharm. 2008; 70:697. [PubMed: 18655830]
18. Sun LQ, Qin B, Huang L, Qian K, Chen CH, Lee KH, Xie L. Bioorg Med Chem Lett. 2012; 22:2376. [PubMed: 22406117]
19. Sun LQ, Zhu L, Qian K, Qin B, Huang L, Chen CH, Lee KH, Xie L. J Med Chem. 2012; 55:7219. [PubMed: 22856541]
20. Janssen PAJ, Lewi PJ, Arnold E, Daeyaert F, de Jonge M, Heeres J, Koymans L, Vinkers M, Guillemont J, Pasquier E, Kukla M, Ludovici D, Andries K, de Bethune MP, Pauwels R, Das K, Clark AD Jr, Frenkel YV, Hughes SH, Medaer B, De Knaep F, Bohets H, De Clerck F, Lampo A, Williams P, Stoffels P. J Med Chem. 2005; 48:1901. [PubMed: 15771434]
21. Baka E, Comer JEA, Takács-Novák K. J Pharm Biomed Anal. 2008; 46:335. [PubMed: 18055153]
22. Jorgensen WL, Duffy EM. Adv Drug Deliv Rev. 2002; 54:355. [PubMed: 11922952]
23. Frenkel YV, Clark AD Jr, Das K, Wang YH, Lewi PJ, Janssen PAJ, Arnold E. J Med Chem. 2005; 48:1974. [PubMed: 15771441]
24. Saxena BB, Han YA, Fu D, Rathnam P, Singh M, Laurence J, Lerner S. AIDS. 2009; 23:917. [PubMed: 19381077]
25. Das K, Bauman JD, Clark AD Jr, Frenkel YV, Lewi PJ, Shatkin AJ, Hughes SH, Arnold E. Proc Natl Acad Sci USA. 2008; 105:1466. [PubMed: 18230722]
26. Khalili F, Henni A, East ALL. J Chem Eng Data. 2009; 54:2914.

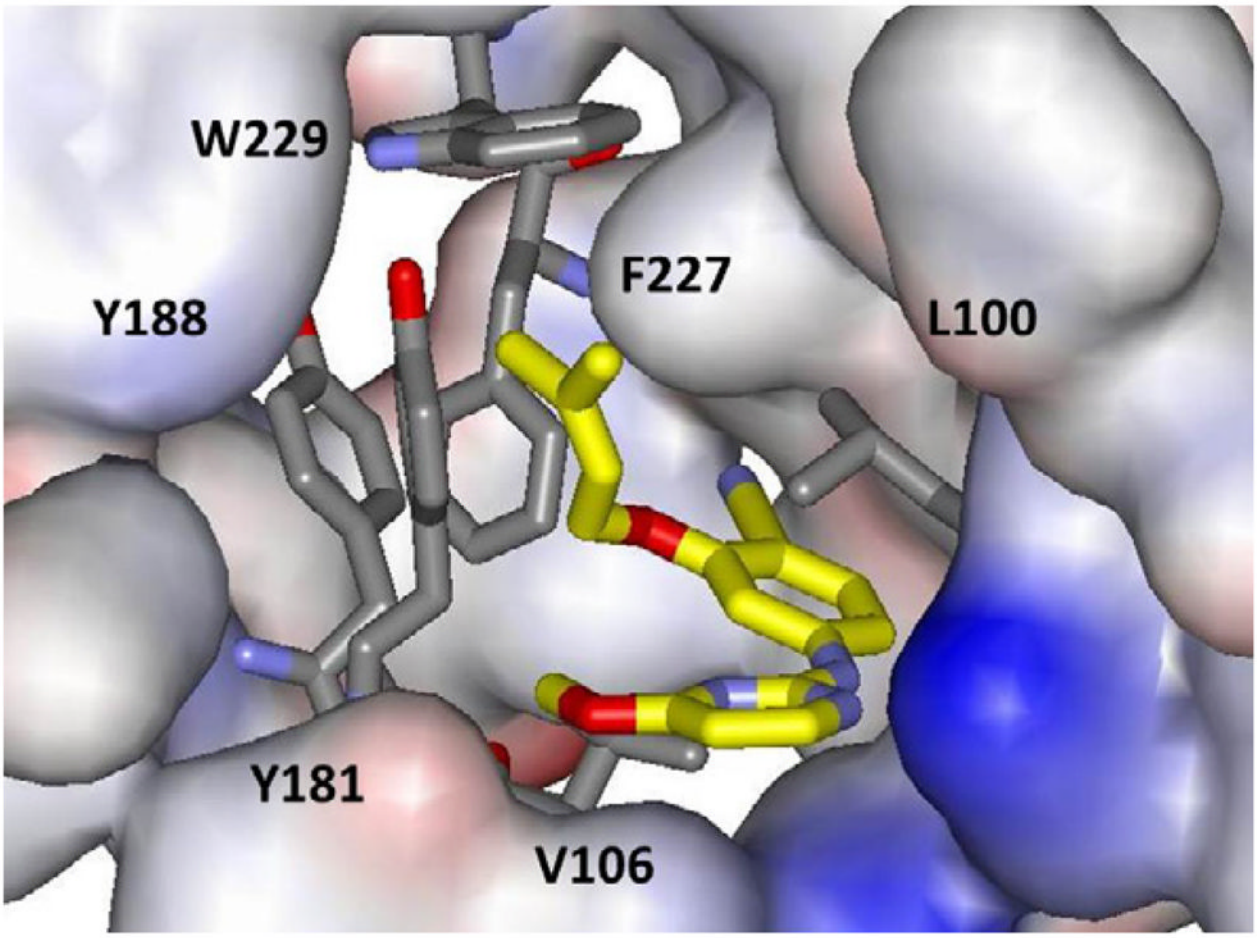

Figure 1.
Rendering of the 1.95-Å crystal structure of **1** with WT HIV-RT. Carbon atoms of **1** are in yellow. Some residues are omitted for clarity.

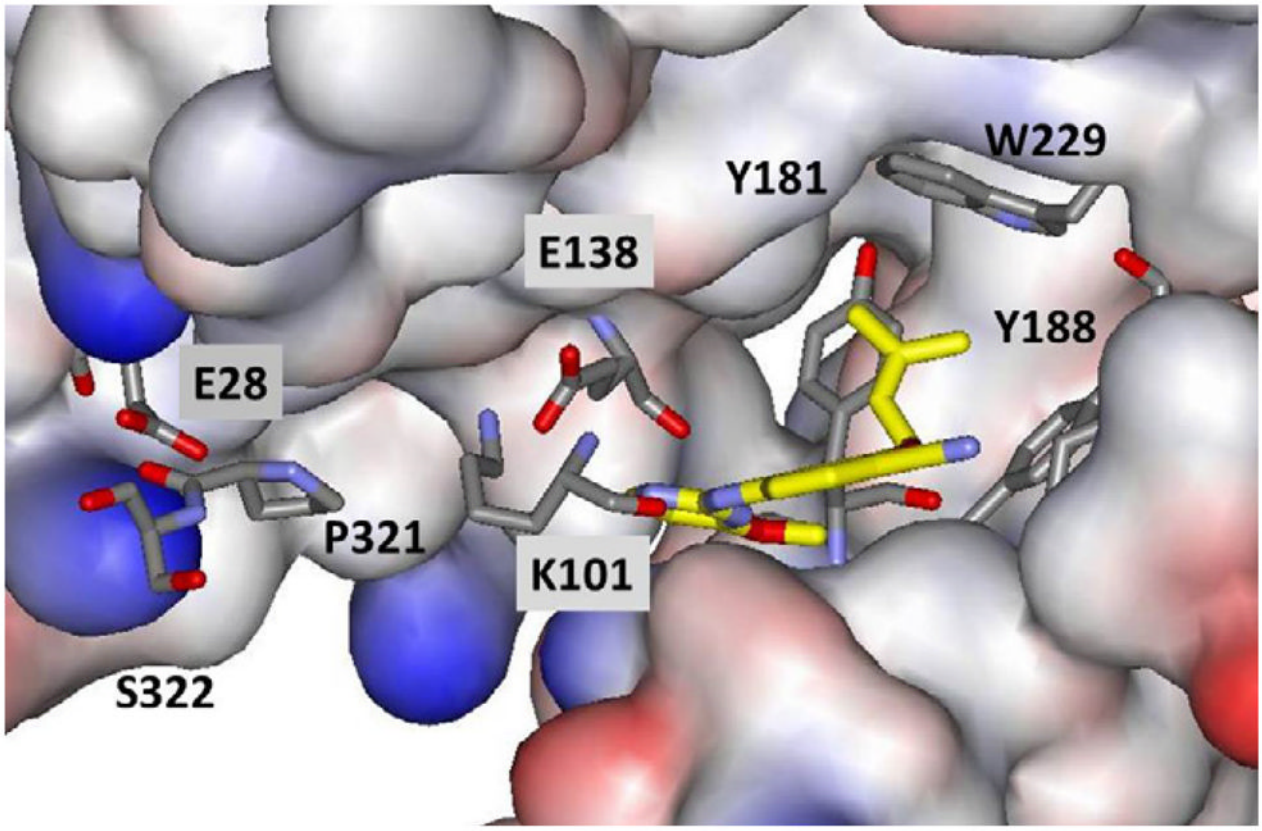

Figure 2.
View from the right in Figure 1 of the crystal structure of **1** bound to WT HIV-RT. Some residues are omitted for clarity. Coordinates have been deposited in the PDB as structure 4KO0.

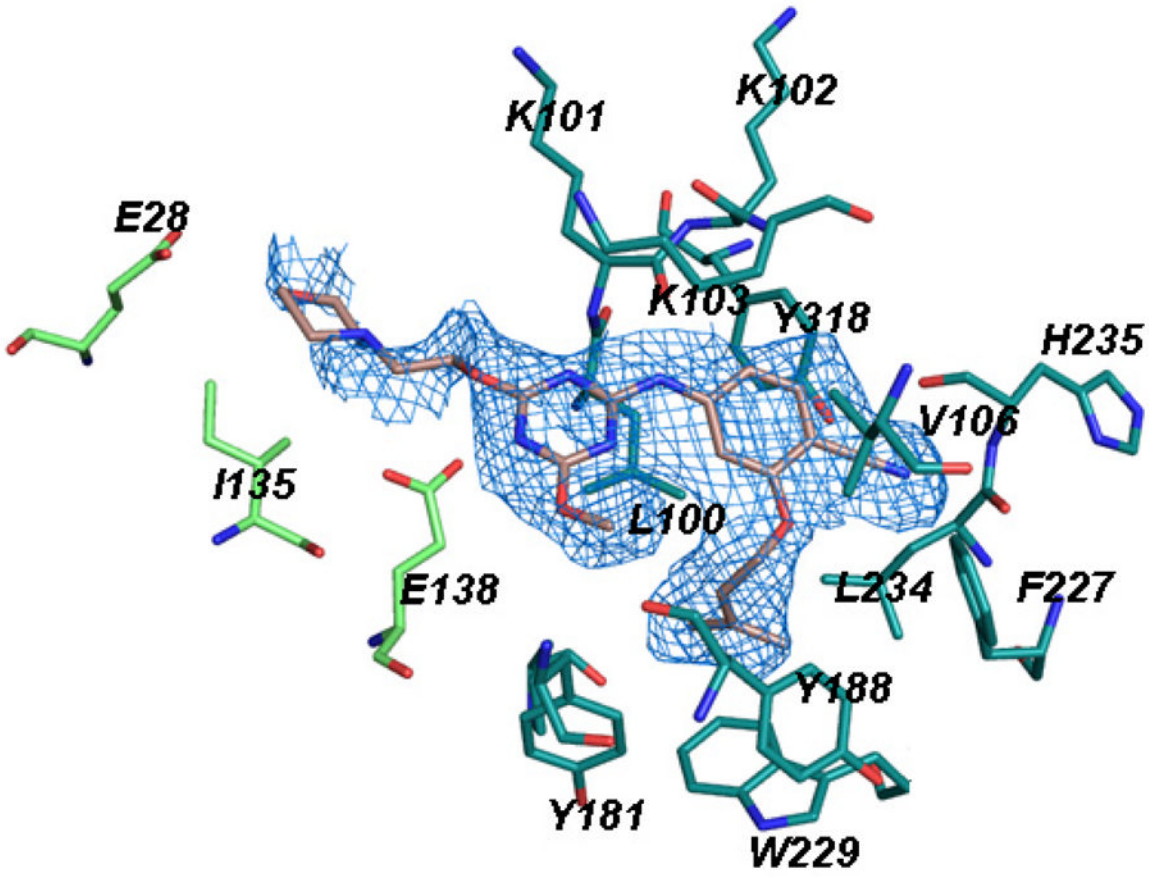

Figure 3.
Omit $F_o - F_c$ electron density map at a contour level of $^{3.0}\sigma$ showing **2j** in the NNRTI binding site of HIV-1 RT with extension towards Glu28 in the entrance channel.

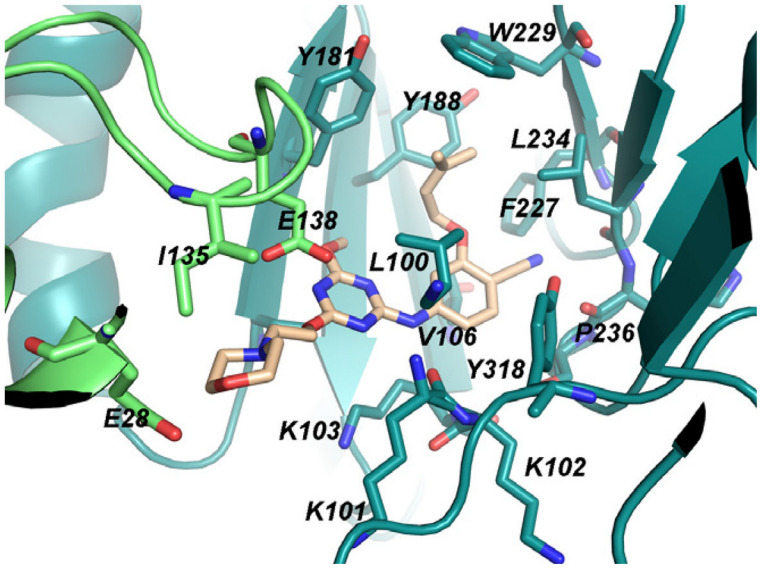

Figure 4.
Illustration of the crystal structure of **2j** with HIV-1 RT; the morpholinoethoxy side chain projects towards Glu28B. Coordinates have been deposited in the PDB as structure 4KKO.

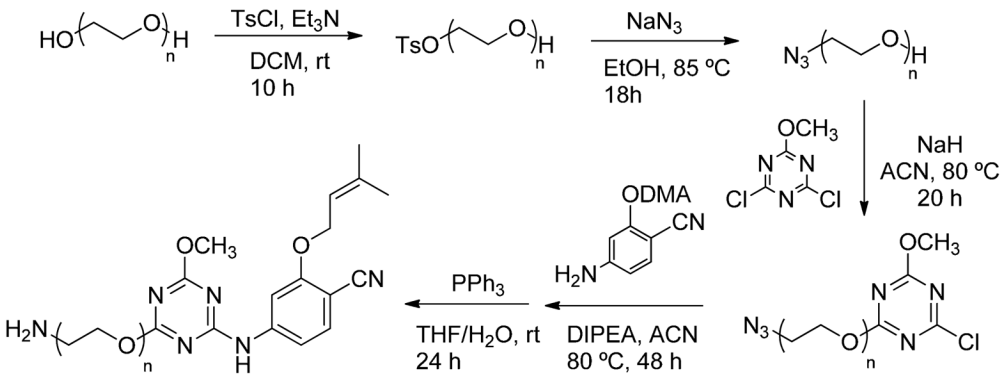

Scheme 1.
Synthesis of **2f** and **2g**.

Table 1

Anti-HIV-1 Activity (EC_{50}) and cytotoxicity (CC_{50}), μM[a]

Compound	R	R′	EC_{50}	CC_{50}
2a[b]	OCH_3	H	0.011	42
2b[b]	OCH_3	OCH_3	0.022	>100
2c[c]	OCH_3	$OCH_2CH_2OCH_3$	0.097	8.6
2d[c]	CH_2CH_3	$OCH_2CH_2OCH_3$	0.057	2.1
2e[c]	OCH_3	$(OCH_2CH_2)_3OCH_3$	0.380	4.2
2f	OCH_3	$(OCH_2CH_2)_4NH_2$	2.2	23
2g	OCH_3	$(OCH_2CH_2)_6NH_2$	5.0	18
2h[c]	OCH_3	OCH_2CH_2-4-MePiz	0.320	7.0
2i[c]	OCH_3	OCH_2CH_2-2-THP	1.2	4.2
2j	OCH_3	OCH_2CH_2-Morph	0.092	2.5
2k	OCH_3	$OCH_2CH_2CH_2$-Morph	0.095	3.6
2l	CH_2CH_3	OCH_2CH_2-Morph	0.150	0.8
2m	c-C_3H_5	OCH_2CH_2-Morph	0.100	0.9
2n	OCH_3	$OCH_2CH_2CH_2$-4-Pip	1.500	5.6
nevirapine			0.110	>100
efavirenz			0.002	15
rilpivirine			0.001	8

[a] 4-MePiz = *N*-methylpiperazinyl; 2-THP = 2-tetrahydropyranyl (racemic); Morph = *N*-morpholinyl; Pip = piperidinyl.

[b] Ref. 10.

[c] Ref. 16.

Table 2

Aqueous Solubility at pH 6.5 (S)

Compound	S, μg/mL	Compound	S, μg/mL
2a	0.1	efavirenz	68.0
2j	42.2	dapivirine	0.15
2k	52.3	rilpivirine	0.24[a], 0.02[b]

[a] Ref. 18, pH 7.4.

[b] Ref. 20, pH 7.